Published in final edited form as:
J Comp Neurol. 2011 November 1; 519(16): 3128–3138. doi:10.1002/cne.22720.

A Novel Type of Complex Ganglion Cell in Rabbit Retina

Benjamin Sivyer[1,*], **Sowmya Venkataramani**[2], **W. Rowland Taylor**[2], and **David I. Vaney**[1]

[1]ARC Centre of Excellence in Vision Science, Queensland Brain Institute, The University of Queensland, Brisbane, Queensland 4072, Australia

[2]Department of Ophthalmology, Casey Eye Institute, Oregon Health and Science University, Portland, Oregon 97239

Abstract

The 15–20 physiological types of retinal ganglion cells (RGCs) can be grouped according to whether they fire to increased illumination in the receptive-field center (ON cells), decreased illumination (OFF cells), or both (ON-OFF cells). The diversity of RGCs has been best described in the rabbit retina, which has three types of ON-OFF RGCs with complex receptive-field properties: the ON-OFF direction-selective ganglion cells (DSGCs), the local edge detectors, and the uniformity detectors. Here we describe a novel type of bistratified ON-OFF RGC that has not been described in either physiological or morphological studies of rabbit RGCs. These cells stratify in the ON and OFF sublaminae of the inner plexiform layer, branching at about 30% and 60% depth, between the ON and OFF arbors of the bistratified DSGCs. Similar to the ON-OFF DSGCs, these cells respond with transient firing to both bright and dark spots flashed in the receptive field but, unlike the DSGCs, they show no directional preference for moving stimuli. We have termed these cells “transient ON-OFF” RGCs. Area-response measurements show that both the ON and the OFF spike responses have an antagonistic receptive-field organization, but with different spatial extents. Voltage-clamp recordings reveal transient excitatory inputs at light ON and light OFF; this excitation is strongly suppressed by surround stimulation, which also elicits direct inhibitory inputs to the cells at light ON and light OFF. Thus the receptive-field organization is mediated both within the presynaptic circuitry and by direct feed-forward inhibition.

Keywords

retinal ganglion cell; ON-OFF cell; spike recording; voltage-clamp recording

The first recordings from retinal ganglion cells (RGCs), made by Hartline (1938) with the frog retina, revealed that some RGCs respond to increases in illumination (ON RGCs), some to decreases in illumination (OFF RGCs), and some to both increases and decreases (ON-OFF RGCs). Early recordings in the cat retina made by Kuffler (1953) showed that the ON RGCs and OFF RGCs have a concentric receptive-field organization, with ON-center cells having an OFF-surround, and vice versa, but did not reveal any type of RGC that gives both ON and OFF responses to center stimulation. However, later recordings in the rabbit retina made by Barlow and Hill (1963) identified a type of ON-OFF RGC that gives direction-selective responses to moving stimuli. Levick (1967) subsequently characterized a nondirectional type of ON-OFF RGC in the rabbit retina, termed the “local edge detector,”

[*]CORRESPONDENCE TO: Benjamin Sivyer, PhD, Queensland Brain Institute, The University of Queensland, Brisbane, Queensland 4072, Australia. b.sivyer@uq.edu.au.

which gives sustained responses to small objects of either contrast in its receptive field; it now appears that the local edge detector is the most common type of RGC in lagomorph and rodent retinas (van Wyk et al., 2006). Levick (1967) also described an unusual type of ON-OFF RGC, the uniformity detector, whose maintained firing is suppressed by both ON and OFF stimuli.

Parallel processing in the retina begins at the first synapse in the outer plexiform layer, where information about increases in illumination (light ON) and decreases in illumination (light OFF) is divided into separate bipolar cell pathways (Werblin and Dowling, 1969; Kaneko, 1970). The ON and OFF signals are relayed to the inner plexiform layer (IPL), where the axon terminals of the ON and OFF bipolar cells stratify in different sublaminae (Famiglietti and Kolb, 1976; Famiglietti et al., 1977; Euler et al., 1996): the OFF bipolar cells terminate closer to the inner nuclear layer (INL) in sublamina a (strata 1 and 2, 1–40% depth of the IPL), whereas the ON bipolar cells terminate closer to the ganglion cell layer (GCL) in sublamina b (strata 3–5, 40–100% depth of the IPL). Since the stratification level of the ganglion cell dendrites determines the bipolar cell input, it also predicts the polarity of responses to light stimuli (Nelson et al., 1978). Thus ON-OFF RGCs tend to be bistratified, with dendrites in both sublamina a and sublamina b of the IPL. For example, the ON-OFF direction-selective ganglion cells (DSGCs) branch at about 20% and 70% depth of the IPL (Amthor et al., 1984; Famiglietti, 1992). The ON-OFF uniformity detectors are also bistratified neurons (Amthor et al., 1989), but they branch closer to the edges of the IPL, at about 10% and 80% depth (Sivyer et al., 2010). By contrast, dye injection revealed that the ON-OFF local edge detectors are monostratified neurons, branching at about 40% depth (Amthor et al., 1989; van Wyk et al., 2006). However, the local edge detectors stratify at the border of the sublaminae and thus are appropriately positioned for a monostratified RGC to receive input from both ON and OFF bipolar cells.

An extensive morphological study of RGCs in the rabbit retina identified only two types of bistratified RGCs, the G7 cell and the G3 cell (Rockhill et al., 2002). The G7 cell clearly has the distinctive dendritic morphology of the ON-OFF DSGC. The G3 cell resembles a type of bistratified RGC that responds only to increases in illumination (Roska and Werblin, 2001; Roska et al., 2006), but the correspondence is equivocal. This “ON-bistratified” RGC appears equivalent both physiologically and morphologically to the “diving bistratified” RGC described recently by Hoshi et al. (2009). In the work described here, we identified a novel type of complex RGC, here termed the “transient ON-OFF” RGC, whose receptive-field properties and dendritic morphology are distinct from those of other types of RGCs previously described in the rabbit retina.

MATERIALS AND METHODS

Experiments conducted in Brisbane, Queensland, were performed in accordance with the Australian Code of Practice, and the experimental protocols were approved by the Animal Ethics Committee of The University of Queensland. Experiments conducted in Portland, Oregon, were in accordance with the National Institutes of Health guidelines, and the experimental protocols were approved by the Institutional Animal Care and Use Committee at Oregon Health and Science University. The procedures have been described in detail previously (Taylor and Vaney, 2002; Sivyer and Vaney, 2010).

Experiments were performed on adult pigmented Dutch-belted rabbits of either sex, which were anesthetized with 40 mg/kg ketamine and 40 mg/kg xylazine (i.m.) before being administered an overdose of 150 mg/kg pentobarbitone sodium (i.v.). After this overdose, the eyes were quickly enucleated and hemisected, and the eyecups placed in Ames medium gassed with carbogen (95% O_2, 5%CO_2) at room temperature (pH 7.4). Under infrared (IR)

illumination, the inferior portion of the eyecup was cut in two, and forceps were used to grasp the myelinated band and peel the retina from the underlying sclera. The retina was then positioned photoreceptor side down in a tissue chamber, held in place with a grid, and mounted under an Olympus BX-51 WI microscope. The dual-port microscope was used with a ×20 0.95-NA objective, allowing both visual stimulation of a large retinal field of ~1.2 mm diameter at ×20 magnification and IR visualization of a smaller field of 110 × 85 μm at ×80 magnification using gradient-contrast optics (Dodt et al., 1999).

RGCs with a small, round soma were targeted for recording, and, after we had made a small hole in the inner limiting membrane, an electrode containing Ames medium was advanced onto the soma. The receptive-field properties of RGCs that fired in response to both ON and OFF stimuli were then analyzed in more detail (see below).

After physiological characterization of the spike responses of four of the transient ON-OFF RGCs, another electrode containing 2% Neurobiotin (Vector Laboratories, Burlingame, CA) was applied to the soma, and the cell was labeled by semiloose-seal electroporation of Neurobiotin (Kanjhan and Vaney, 2008). In one experiment, an ON-OFF DSGC overlapping the Neurobiotin-filled cell was patch-clamped with an electrode containing 0.5% Lucifer yellow in an intracellular solution (125 mM methanesulfonic acid, 5 mM Na-HEPES, 1 mM EGTA, 3 mM Mg-ATP, 0.3 mM Tris-GTP, 10 mM phosphocreatine, balanced to pH 7.2 with KOH). The retina was fixed for 30 minutes in 4% paraformaldehyde in 0.1 M phosphate buffer and washed overnight in 0.1 M phosphate-buffered saline (PBS). It was then incubated for 5–7 days in 0.1 M PBS containing 2% bovine serum albumin (Jackson Immunoreserarch, West Grove, PA; IgG-free BSA), 1% normal donkey serum (Jackson Immunoreserarch), 0.1% Triton X-100, and either anticalbindin D-28k or anti-Lucifer yellow. After this, the retina was again washed overnight in 0.1 M PBS before being incubated overnight in streptavidin conjugated to Cy3 (Jackson Immunoreserarch; 1:500) and anti-rabbit IgG conjugated to Cy2 or Cy5 (Jackson Immunoreserarch; 1:500). Each step was performed at room temperature (~22°C).

The antibodies used in this study are listed in Table 1, and their labeling patterns matched those described in previous studies on rabbit retina. The rabbit polyclonal antibody against calbindin labels a single band of 28 kDa in brain homogenates from wild-type mice but not from calbindin-knockout mice (Airaksinen et al., 1997). In rabbit retina, the anticalbindin D-28K labels the horizontal cells and populations of bipolar cells and amacrine cells (Mitchell et al., 1995; Massey and Mills, 1996); the same pattern of labeling was seen in this study. The rabbit polyclonal antibody against Lucifer yellow (Invitrogen, Carlsbad, CA; A-5750; previously marketed as Molecular Probes A-5750; http//antibodyregistry.org/AB_1501344) has been used in previous studies to intensify neurons filled with Lucifer yellow (Taghert et al., 1982; Naritsuka et al., 2009). The pattern of Lucifer immunofluoresence was identical to the natural fluorescence of the injected dye, but brighter and resistant to fading; only the RGC injected with Lucifer showed Lucifer immunofluoresence (Sivyer and Vaney, 2010).

Fluorescent-labeled tissue was imaged with a Zeiss LSM 510 Meta confocal microscope, and LSM files were imported into ImageJ for further processing. Side projections were made using the 3D Project tool, and bi- and tricolor depth coding were achieved by combining the z-sections through the ON sublamina in one projection (typically five 0.4-μm sections at ×63 magnification) and the remaining section(s) in another projection, using the Z-Project tool. The projections were then pasted into separate color channels in Adobe Photoshop. Contrast and brightness were adjusted in Adobe Photoshop.

The stratification levels of labeled neurons were mapped by measuring the variation in mean fluorescence with retinal depth for small columns of retina, either 10 μm square or 20 μm square, within a confocal stack extending from the GCL to the INL in 0.2-μm increments; 15–20 such columns were averaged to produce the stratification graphs. The absolute depth of branching was set relative to the known stratification levels of either the ON-OFF DSGCs, which branch at ~20% and ~70% depth of the IPL (Famiglietti, 1992), or the CBb5 bipolar cells, which branch at about 83% depth (Massey and Mills, 1996; MacNeil et al., 2004).

Recording electrodes were pulled from borosilicate glass to a resistance of 3–5 MΩ. Extracellular electrodes were filled with Ames medium, and patch electrodes for voltage-clamp recordings were filled with the following: 125 mM Cs-methanesulfonate, 5 mM Na-HEPES, 1 mM EGTA, 3 mM Mg-ATP, 0.3 mM Tris-GTP, 10 mM phosphocreatine, 5 mM TEA-Cl, and 3 mM lidocaine N-ethyl chloride (QX-314), balanced to pH 7.2 with CsOH. Cs^+ was used to block voltage-gated K^+ channels and thereby improve the voltage clamp at more positive potentials, whereas QX-314 blocked voltage-gated Na^+ channels and abolished all spiking activity less than 1 minute after establishing the whole-cell configuration. The measured liquid junction potential of 10 mV was subtracted from all traces, and the series resistance was not routinely compensated for online.

The calculation of the excitatory and inhibitory components of the light-evoked synaptic inputs has been described in detail previously (Borg-Graham, 2001; Taylor and Vaney, 2002). Briefly, the visual stimulus was repeated while voltage clamping the RGCs at a range of potentials from −90 mV to −10 mV in 10-mV increments. The resting current–voltage (IV) relation was measured 100–200 msec prior to the onset of the light stimulus. To obtain the net light-evoked conductance as a function of time, the leak IV was subtracted from IVs measured every 10 msec for the duration of the light stimulation. The total light-evoked conductance change was estimated from the slope of the linear regression fit to each IV. The total conductance was assumed to comprise the sum of linear excitatory and inhibitory conductance components with reversal potentials of 0 mV and −65 mV, respectively.

Visual stimuli were generated using custom software (Igor Pro) and presented at 75 Hz on an organic light-emitting diode screen (eMagin OLED-XL microdisplay, peak 518 nm). The stimuli were projected through the microscope and focused onto the photoreceptor outer segments with a ×20 objective (0.95 NA). In most experiments, the background illumination was maintained above the level of rod saturation at ~3.5 e^{11} quanta/cm^2/second, and the visual stimuli were set at ± 80% of the background (1.75 e^{11} quanta/cm^2/second for OFF stimuli; 5.25 e^{11} quanta/cm^2/second for ON stimuli).

To test whether RGCs were direction selective, extracellular action potentials were recorded in response to 12 stimulus directions at 30° intervals. A direction-selectivity index (DSI) was used as a measure of the directional tuning and was calculated as follows: the response in each direction was represented as a vector, pointing in the direction of the stimulus and having length equal to the number of spikes recorded during that stimulus (Taylor and Vaney, 2002). The DSI was equal to the normalized length of the vector sum of the responses in all 12 directions. Thus defined, the DSI would range from 0, when the responses were equal in all stimulus directions, to 1, when a response is obtained only for a single stimulus direction.

RESULTS

Targeting and identification of RGCs

The somata of RGCs in the visual streak of the rabbit retina were targeted for loose-seal recording of their action potentials under IR control. Each cell was tested with a small spot of 200 μm diameter flashed in the middle of the receptive field to determine whether it responded to illumination increases (ON cell) or decreases (OFF cell). A small proportion of RGCs fired at both phases of illumination, indicating that they were ON-OFF cells. These included RGCs with a large soma that fired transiently at light ON and light OFF; stimulation with moving bars of light showed that they responded preferentially to movement in one direction, characteristic of the ON-OFF DSGCs. Other RGCs with smaller somata also fired at both light ON and light OFF. These included cells with receptive-field properties matching the previously characterized local edge detectors; unlike other types of ON-OFF RGCs, the local edge detectors showed sustained firing at both light ON and light OFF in response to a small flashing spot (van Wyk et al., 2006).

Another type of ON-OFF RGC with a small soma gave transient responses to flashing stimuli, and here we call them “transient ON-OFF” RGCs. The success rate for recording from transient ON-OFF RGCs was increased by targeting small, round somata while avoiding more elongated somata with an eccentric nucleus characteristic of local edge detectors (Fig. 1; van Wyk et al., 2006).

Transient ON-OFF RGCs could be distinguished physiologically from local edge detectors by the duration of their responses to light steps: the transient ON-OFF RGCs fired spikes for about 100 msec, whereas the local edge detectors responded for seconds (Fig. 2; van Wyk et al., 2006). The duration of spiking responses in local edge detectors and transient ON-OFF RGCs was compared by measuring the time after a light step at which 80% of the spikes had occurred. For a dark centered spot of 200 μm diameter flashed for 2 seconds, 80% of the spikes occurred within ~100 msec of the contrast transition for both the OFF and the ON responses (OFF 90 ± 40 msec, ON 60 ± 30 msec, n = 7). By contrast, under identical recording conditions, the step responses of the local edge detectors were significantly more sustained: 80% of the spikes occurred after 1.2 ± 0.1 seconds for the OFF response and 3.3 ± 0.1 seconds for the ON response (n = 5, $P < 0.001$).

Responses to moving stimuli

ON-OFF DSGCs are commonly encountered in the rabbit retina and, like the ON-OFF transient RGCs, respond transiently to both flashing and moving stimuli (Barlow et al., 1964). However, the transient ON-OFF RGCs could be readily distinguished from the DSGCs by the lack of directional preference. A dark bar (200 × 500 μm), moving parallel to the long axis at 1,000 μm/second in 12 directions produced bursts of spikes as the leading and trailing edges passed over the receptive field, with slightly more spikes being elicited by the trailing edge (Fig. 3). None of the transient ON-OFF RGCs tested was strongly direction selective: the mean DSI for the leading OFF response was 0.09 ± 0.06, whereas that for the trailing ON response was 0.05 ± 0.02 (n = 7). The preferred directions calculated for the ON and OFF components of the transient ON-OFF RGCs were uncorrelated. By contrast, ON-OFF DSGCs tested using a comparable stimulus had an OFF DSI of 0.55 ± 0.12 and an ON DSI of 0.57 ± 0.08 (Taylor and Vaney, 2002).

Dendritic morphology and stratification

After the physiological characterization of spike responses, four of the transient ON-OFF RGCs were labeled with Neurobiotin. Confocal reconstructions revealed that the small soma (diameter: 13.7 ± 0.7 μm, n = 4) gave rise to three primary dendrites, which formed a

densely branched tree containing many short terminal dendrites, 5–10 μm long (Fig. 4A). The preterminal and terminal dendrites often crossed and bore numerous small dendritic spines. Like most RGCs in the visual streak, the soma was positioned asymmetrically within the dendritic field, near its dorsal margin. At first glance, the dendrites appeared to be broadly stratified within the middle of the IPL, but careful examination under high magnification revealed that the transient ON-OFF RGCs were actually bistratified (Fig. 4B). The primary dendrites coursed through the IPL to branch at a level just proximal to the most distal stratification; the dendrites then branched distally in the OFF sublamina and returned to branch proximally in the ON sublamina. These recurrent dendrites traversed the space between dendritic strata almost vertically and usually terminated without further branching (Fig. 4C).

One retina containing a Neurobiotin-filled transient ON-OFF RGC was also stained with a calbindin antibody to label the CBb5 bipolar cells, the axon terminals of which stratify near the border of strata 4 and 5 (Fig. 5A). The transient ON-OFF RGCs branched distal to the CBb5 terminals, with the ON arbor at the border of strata 3 and 4, and the OFF arbor in the middle of stratum 2. Stratification of the dendritic arbors could be delineated more clearly in another preparation in which a Neurobiotin-labeled transient ON-OFF RGC overlapped a Lucifer-labeled ON-OFF DSGC (Fig. 5B). The ON-OFF DSGCs are narrowly bistratified, branching in the middle of stratum 4 and at the border of strata 1 and 2, at the same levels as the ON and OFF cholinergic amacrine cells, respectively (Famiglietti, 1992). As expected, both the proximal and distal arbors of the transient ON-OFF RGC were located between the arbors of the DSGC: the ON arbors of the two cell types abutted each other, as did the OFF arbors, with a space in between that was relatively free of dendrites.

The relative stratification levels were confirmed by quantitative measurement of the fluorescence intensity, as described in Material and Methods, with the peak fluorescence of the OFF and ON arbors of the DSGC being set at 20% and 70% depth of the IPL, respectively (Fig. 5C). By comparison, the OFF and ON arbors of the transient ON-OFF RGC peaked at about 30% and 60% depth, respectively. Consequently, the separation of the two arbors of the transient ON-OFF RGC (~30% depth) was much less than that of the two arbors of the ON-OFF DSGC (~50% depth).

Dendritic-field size

The dendritic-field size of RGCs in the rabbit retina increases rapidly with decreasing RGC density from the peak visual streak. Consequently, in the absence of a large sample of filled cells at different eccentricities from the visual streak, it is difficult to establish how the dendritic-field size of the ON-OFF transient RGCs compares with that of other medium-field RGCs in the rabbit retina. However, dual labeling of a pair of overlapping cells allowed the novel transient ON-OFF RGC to be compared directly with the well characterized ON-OFF DSGC (Fig. 5D). The equivalent dendritic-field diameter of the transient ON-OFF RGC was 223 μm for the ON arbor and 228 μm for the OFF arbor, whereas the ON-OFF DSGC had a dendritic-field diameter of 207 μm for both the ON and the OFF arbors. Thus the dendritic-field area of each arbor of the ON-OFF transient RGC was ~1.2 times greater than the corresponding arbor of the DSGC. Measurements of all three transient ON-OFF RGCs that were filled with Neurobiotin confirmed that the ON arbor (219 ± 9 μm diameter) was equivalent in size to the OFF arbor (220 ± 16 μm diameter).

Surround responses

The area–response function of seven transient ON-OFF RGCs was measured by stimulating the cells with a series of dark spots, 50–1,000 μm diameter, which were centered on the soma (Fig. 6A). Raster plots from a single cell show the spike responses to multiple

presentations of the stimuli (Fig. 6B); characteristically, the ON response was larger than the OFF response for all but the smallest spots, as seen with moving stimuli. The cell did not respond to a 50-μm spot, but gave a strong OFF response to a 100-μm spot, which covered only 20% of the dendritic-field area. Spots from 150 to 400 μm in diameter elicited both ON and OFF responses, whereas larger spots elicited only weak ON responses. These differences in the spatial tuning of the ON and OFF responses were consistent across the seven cells, as shown by the averaged data (Fig. 6C). Both the ON and the OFF area responses are well fitted with difference-of-Gaussians (DOG) functions, but they differed in two ways. First, the size of the excitatory center of the receptive field, as estimated from the peak of the DOG fit to the data (Fig. 6C), was smaller for the OFF response than the ON response (OFF center = 110 ± 29 μm, ON center = 201 ± 41 μm, n = 7, $P < 0.01$). Second, the tuning width of the inhibitory surround was narrower for the OFF response than the ON response (OFF DOG width = 222 ± 56 μm, ON DOG width = 372 ± 102 μm, n = 7, $P < 0.05$).

Whole-cell recordings were made from transient ON-OFF RGCs to investigate the excitatory and inhibitory synaptic inputs that underlie the spatial tuning of the ON and OFF spike responses (Fig. 6D–I). A dark spot flashed over the soma for 2 seconds generated transient excitatory input at both light OFF and light ON, indicating input from both OFF and ON bipolar cells. In agreement with the spike responses, the light-evoked excitatory conductance was largest for the 200-μm spot, which about corresponds to the dendritic-field diameter of the transient ON-OFF RGCs in the visual streak. Both the ON and the OFF excitatory inputs were suppressed by the 800-μm spot (ON by 59 ± 24%, OFF by 70 ± 17%, n = 10), which also elicited the largest direct inhibitory input. These results indicate that the surround is generated by both a reduction in the excitatory drive from bipolar cells and an increase in direct inhibitory input, in both the ON and the OFF sublaminae of the IPL. Although the conductance analysis is consistent with the overall decrease in spike responses with increasing surround stimulation, the data do not account for the differences in optimal spot size for the ON and OFF spike responses (Fig. 6C).

DISCUSSION

Transient ON-OFF RGCs

We have characterized a novel type of RGC, the transient ON-OFF RGC, which has not been identified previously. These cells were consistently encountered, alongside known ON-OFF RGCs, including the ON-OFF DSGCs, local edge detectors, and uniformity detectors (Fig. 7). The cells fire transiently to both ON and OFF stimuli, and their dendritic trees are closely bistratified at about 30% and 60% depth of the IPL, in the OFF and ON sublaminae, respectively. Patch-clamp recordings showed that the transient spike responses of these cells are largely shaped by transient excitatory inputs at both light ON and light OFF, presumably from populations of ON and OFF bipolar cells. Because ON-OFF DSGCs, which stratify closer to the margins of the IPL, also receive transient excitatory inputs, these results indicate that transient release from bipolar cells occurs throughout much of the IPL, contrary to the notion that there is an ordered transient-sustained lamination (Roska and Werblin, 2001).

We cannot discount the possibility that the transient ON-OFF RGCs might have been encountered in previous physiological studies and classified as local edge detectors on the basis of their nondirectional ON-OFF responses, although local edge detectors have smaller receptive fields and show relatively sustained firing to standing contrast. Moreover, the transient ON-OFF RGCs may correspond to the single “edge-detector” RGC encountered by Vaney et al. (1981). They could also be mistaken for ON-OFF DSGCs if not tested with

appropriate moving stimuli, but their dendritic morphology is clearly different from that of both the ON-OFF DSGCs and the local edge detectors.

For the overlapping pair of cells injected with Neurobiotin and Lucifer yellow, the dendritic-field area of each arbor of the transient ON-OFF RGC was about 1.2 times larger than that of each arbor of the ON-OFF DSGC. Each of the four subtypes of ON-OFF DSGCs accounts for ~3% of all RGCs in the rabbit retina (Vaney, 1994), suggesting that the transient ON-OFF RGCs might account for ~2.5% of all RGCs, if the two cell types have a similar 1.4-fold dendritic-field overlap. If the transient ON-OFF RGCs have a 3-fold dendritic-field overlap, similar to some other types of RGCs (Wässle et al., 1981; Sivyer and Vaney, 2010), then they might account for ~5% of all RGCs.

The transient ON-OFF RGCs were not recognized in an extensive morphological survey of RGCs in the rabbit retina by Rockhill and colleagues (2002), who could have expected to see 18–37 of these cells in their random sample of 734 RGCs, if the transient ON-OFF RGCs comprise 2.5–5% of all RGCs. However, the small soma might have lead to undersampling of the population, or perhaps the cells were encountered but included with other highly branched morphological types, such as the G4 (beta) ganglion cells, particularly insoifar as the close bistratification is not very apparent in whole-mount view.

Synaptic inputs from the surround

The firing of transient ON-OFF RGCs was progressively suppressed as the stimulus extended beyond the dendritic field, and the area–response profile was well described by a DOG function. Although the ON dendritic field was similar in size to the OFF dendritic field, the spatial tuning of the ON and OFF receptive fields differed markedly: the OFF response had a smaller center and surround and thus was tuned to higher spatial frequencies than the ON response. Similar to these brisk-transient ON-OFF ganglion cells, the sluggish-sustained ON-OFF local edge detectors also show an asymmetry in the spatial tuning of the ON and OFF responses. The arrangement is reversed for the local edge detectors, however, the surround for the ON response being narrower than that for the OFF response (van Wyk et al., 2006). The functional rationale for having different spatiotemporal filtering properties for these RGCs remains obscure.

Conductance analysis suggested that the synaptic mechanisms producing the spatial tuning were similar for the ON and the OFF responses. Surround stimulation produced both a presynaptic reduction in excitatory drive and postsynaptic feed-forward inhibition. It is interesting to note that feed-forward surround inhibition is seen in both the transient ON-OFF RGCs and the ON-OFF DSGCs (Taylor and Vaney, 2002), both of which can be classified as brisk-transient ON-OFF cells. In contrast, the surround of the local edge detectors, which are sluggishly sustained ON-OFF cells, is mediated entirely by presynaptic inhibition (van Wyk et al., 2006). What is not clear for each type of RGC is how much of the inhibitory surround is generated in the outer retina and how much in the inner retina. Further analysis will be needed to determine how the spatial arrangement of the excitatory and inhibitory synaptic inputs generates the different spatial dimensions of the OFF and ON responses in the diverse types of ON-OFF RGCs.

Comparison with other species

Although there are no previous descriptions of the transient ON-OFF RGCs in the rabbit retina, a number of other mammalian retinae contain RGCs that appear to be morphologically homologous. The “theta” cell of the cat retina appears to be both morphologically and physiologically similar to the transient ON-OFF RGC (Isayama et al., 2000). Both cell types have a small soma and a highly branched dendritic tree that is closely

bistratified in the middle of the IPL. Isayama et al. (2000) noted that the dendritic tree of theta cells "on cursory inspection could be mistaken for a broadly unistratified arbor centred on the a/b sublamina border" and, likewise, our initial inspections of the transient ON-OFF RGCs led us to believe that they were broadly monostratified. Both the transient ON-OFF RGC and the theta cell are bistratified at about the same levels in the IPL, and the ON and OFF dendritic arbors are joined by vertical branches in both cells. Finally, preliminary recordings in the cat retina suggest physiological similarities, in that the theta cell responds transiently to ON and OFF stimuli (O'Brien et al., 1999).

It is possible that the transient ON-OFF RGCs are homologous to the "broad thorny" cells in the primate retina, which branch in the middle of the IPL (Dacey et al., 2003). Although these cells have not been described as bistratified, their transient ON-OFF responses (Dacey, 2004) suggest that inspection at greater z-axis resolution may reveal a closely spaced bistratification. Indeed, Yamada et al. (2005) proposed that the broad thorny cell is homologous to the theta cell described by Isayama et al. (2000).

Although transient ON-OFF RGCs that are nondirectional have not been reported in physiological studies of the mouse retina, six morphological types of bistratified RGCs have been described (Völgyi et al., 2009), one of which appears to be very similar to the transient ON-OFF RGC in the rabbit retina. This "type-3 bistratified" RGC was first described by Schubert et al. (2005) and corresponds to the "G16" cell of Völgyi et al. (2009). The cell stratifies at about 30% and 56% depth of the IPL, between both the cholinergic bands and the arbors of the "type-2 bistratified" RGC, which is the mouse ON-OFF DSGC. The relative dendritic-field sizes of the type-2 and type-3 bistratified cells in the mouse retina are similar to those of the ON-OFF DSGCs and transient ON-OFF RGCs in the rabbit retina, suggesting that these RGC types may be present in similar proportions in the two species. In summary, the transient ON-OFF RGCs, like the ON-OFF DSGCs, appear to be conserved across a number of diverse mammalian species and thus likely represent a fundamental channel for visual information transmission.

RGC diversity in rabbit retina

The identification of the transient ON-OFF RGC adds to the catalog of rabbit RGCs and increases the number of bistratified RGC types discovered since the extensive morphological study by Rockhill and colleagues (2002). Including the transient ON-OFF RGC, there are now as many as seven morphological types of bistratified RGCs identified in the rabbit, the ON-OFF DSGC (Amthor et al., 1984), the uniformity detector cell (Amthor et al., 1989), a single orientation-selective cell (Amthor et al., 1989), the G3 cell (Rockhill et al., 2002; Hoshi and Mills, 2009), the ON bistratified cell (Roska and Werblin, 2001; Roska et al., 2006; Hoshi et al., 2009), the type 2 bistratified (BS2) cell, and a single type 3 bistratified (BS3) cell (Famiglietti, 2009). This is in good agreement with the four to six types of bistratified RGCs identified in morphological studies of mouse RGCs (Badea and Nathans, 2004; Kong et al., 2005; Coombs et al., 2006; Völgyi et al., 2009). It remains to be determined whether all of the bistratified RGCs in the rabbit retina are ON-OFF cells.

The reasons for the wide diversity of bistratified/ONOFF RGCs in the rabbit and other mammals is unclear; nor is it obvious, for that matter, why 15–20 types of all RGCs are required. Given the similarity in receptive-field size, coverage, and response characteristics, one might expect that there is considerable redundancy in the information conveyed to the brain by the transient ON-OFF RGCs and the four subtypes of DSGCs taken together (Puchalla et al., 2005). Moreover, it is not clear what information is conveyed by the transient ON-OFF RGCs that could not be obtained by combining information from overlapping ON brisk-transient cells and OFF brisk-transient cells. Understanding how the

visual scene is represented by the total activity of numerous diverse populations of RGCs is one of the major outstanding problems in retinal neuroscience (Masland and Martin, 2007).

Acknowledgments

We thank Rowan Tweedale for editing the manuscript and Ilya Buldyrev for helpful suggestions.

Grant sponsor: Australian Research Council; Grant number: CE0561903 (to D.I.V.); Grant sponsor: National Health and Medical Research Council of Australia; Grant number: 511242 (to D.I.V.); Grant sponsor: National Institutes of Health; Grant number: EY014888 (to W.R.T.); Grant sponsor: The University of Queensland (to B.S).

LITERATURE CITED

Airaksinen MS, Eilers J, Garaschuk O, Thoenen H, Konnerth A, Myer M. Ataxia and altered dendritic calcium signalling in mice carrying a targeted null mutation of the calbindin D28k gene. Proc Natl Acad Sci U S A. 1997; 94:1488–1493. [PubMed: 9037080]

Amthor FR, Oyster CW, Takahashi ES. Morphology of on-off direction-selective ganglion cells in the rabbit retina. Brain Res. 1984; 298:187–190. [PubMed: 6722555]

Amthor FR, Takahashi ES, Oyster CW. Morphologies of rabbit retinal ganglion cells with complex receptive fields. J Comp Neurol. 1989; 280:97–121. [PubMed: 2918098]

Badea TC, Nathans J. Quantitative analysis of neuronal morphologies in the mouse retina visualized by using a genetically directed reporter. J Comp Neurol. 2004; 480:331–351. [PubMed: 15558785]

Barlow HB, Hill RM. Selective sensitivity to direction of motion in ganglion cells of the rabbit's retina. Science. 1963; 139:412–414. [PubMed: 13966712]

Barlow HB, Hill RM, Levick WR. Retinal ganglion cells responding selectively to direction and speed of image motion in the rabbit. J Physiol. 1964; 173:377–407. [PubMed: 14220259]

Borg-Graham L. The computation of directional selectivity in the retina occurs presynaptic to the ganglion cell. Nat Neurosci. 2001; 4:176–183. [PubMed: 11175879]

Coombs J, van der List D, Wang GY, Chalupa LM. Morphological properties of mouse retinal ganglion cells. Neuroscience. 2006; 140:123–136. [PubMed: 16626866]

Dacey, DM. Origins of perception: retinal ganglion cell diversity and the creation of parallel visual pathways. In: Gazzaniga, MS., editor. The cognitive neurosciences. 3rd ed.. Cambridge, MA: MIT Press; 2004. p. 281-301.

Dacey DM, Peterson BB, Robinson FR, Gamlin PD. Fireworks in the primate retina: in vitro photodynamics reveals diverse LGN-projecting ganglion cell types. Neuron. 2003; 37:15–27. [PubMed: 12526769]

Dodt H, Eder M, Frick A, Zieglgänsberger W. Precisely localized LTD in the neocortex revealed by infrared-guided laser stimulation. Science. 1999; 286:110–113. [PubMed: 10506556]

Euler T, Schneider H, Wässle H. Glutamate responses of bipolar cells in a slice preparation of the rat retina. J Neurosci. 1996; 16:2934–2944. [PubMed: 8622124]

Famiglietti EV. Dendritic co-stratification of ON and ON-OFF directionally selective ganglion cells with starburst amacrine cells in rabbit retina. J Comp Neurol. 1992; 324:322–335. [PubMed: 1383291]

Famiglietti EV. Bistratified ganglion cells of rabbit retina: neural architecture for contrast-independent visual responses. Vis Neurosci. 2009; 26:195–213. [PubMed: 19272195]

Famiglietti EV, Kolb H. Structural basis for ON- and OFF-center responses in retinal ganglion cells. Science. 1976; 194:193–195. [PubMed: 959847]

Famiglietti EV, Kaneko A, Tachibana M. Neuronal pathways of on and off pathways to ganglion cells in carp retina. Science. 1977; 198:1267–1269. [PubMed: 73223]

Hartline HK. The response of single optic nerve fibers of the vertebrate eye to illumination of the retina. Am J Physiol. 1938; 121:400–415.

Hoshi H, Liu WL, Massey SC, Mills SL. ON inputs to the OFF layer: bipolar cells that break the stratification rules of the retina. J Neurosci. 2009; 29:8875–8883. [PubMed: 19605625]

Isayama T, Berson DM, Pu M. Theta ganglion cell type of cat retina. J Comp Neurol. 2000; 417:32–48. [PubMed: 10660886]

Kaneko A. Physiological and morphological identification of horizontal, bipolar and amacrine cells in goldfish retina. J Physiol. 1970; 207:623–633. [PubMed: 5499739]

Kanjhan R, Vaney DI. Semi-loose seal Neurobiotin electroporation for combined structural and functional analysis of neurons. Pflügers Arch. 2008; 457:561–568.

Kong JH, Fish DR, Rockhill RL, Masland RH. Diversity of ganglion cells in the mouse retina: unsupervised morphological classification and its limits. J Comp Neurol. 2005; 489:293–310. [PubMed: 16025455]

Kuffler SW. Discharge patterns and functional organization of mammalian retina. J Neurophysiol. 1953; 16:37–68. [PubMed: 13035466]

Levick WR. Receptive fields and trigger features of ganglion cells in the visual streak of the rabbits retina. J Physiol. 1967; 188:285–307. [PubMed: 6032202]

MacNeil MA, Heussy JK, Dacheux RF, Raviola E, Masland RH. The population of bipolar cells in the rabbit retina. J Comp Neurol. 2004; 472:73–86. [PubMed: 15024753]

Masland RH, Martin PR. The unsolved mystery of vision. Curr Biol. 2007; 17:R577–R582. [PubMed: 17686423]

Massey SC, Mills SL. A calbindin-immunoreactive cone bipolar cell type in the rabbit retina. J Comp Neurol. 1996; 366:15–33. [PubMed: 8866843]

Mitchell CK, Rowe-Rendelmen CL, Asharaf S, Redburn DA. Calbindin immunoreactivity of horizontal cells in the developing rabbit retina. Exp Eye Res. 1995; 61:691–698. [PubMed: 8846841]

Naritsuka H, Kazuhisa S, Tsutomu H, Kensaku M, Masahiro Y. Perisomatic-targeting granule cells in the mouse olfactory bulb. J Comp Neurol. 2009; 515:409–426. [PubMed: 19459218]

Nelson R, Famiglietti EV, Kolb H. Intracellular staining reveals different levels of stratification for on- and off-center ganglion cells in cat retina. J Neurophysiol. 1978; 41:472–483. [PubMed: 650277]

O'Brien BJ, Isayama T, Berson DM. Light responses of morphologically identified cat ganglion cells. Invest Ophthalmol Vis Sci. 1999; 40 ARVO Abstract 815.

Puchalla JL, Schneidman E, Harris RA, Berry MJ. Redundancy in the population code of the retina. Neuron. 2005; 46:493–504. [PubMed: 15882648]

Rockhill RL, Daly FJ, MacNeil MA, Brown SP, Masland RH. The diversity of ganglion cells in a mammalian retina. J Neurosci. 2002; 22:3831–3843. [PubMed: 11978858]

Roska B, Werblin F. Vertical interactions across ten parallel, stacked representations in the mammalian retina. Nature. 2001; 410:583–587. [PubMed: 11279496]

Roska B, Molnar A, Werblin FS. Parallel processing in retinal ganglion cells: how integration of space-time patterns of excitation and inhibition form the spiking output. J Neurophysiol. 2006; 95:3810–3822. [PubMed: 16510780]

Schubert T, Maxeiner S, Kruger O, Willecke K, Weiler R. Connexin45 mediates gap junctional coupling of bistratified ganglion cells in the mouse retina. J Comp Neurol. 2005; 490:29–39. [PubMed: 16041717]

Sivyer B, Vaney DI. Dendritic morphology and tracer-coupling pattern of physiologically identified transient uniformity detector ganglion cells in rabbit retina. Vis Neurosci. 2010; 27:159–170. [PubMed: 20854715]

Sivyer B, Taylor WR, Vaney DI. Uniformity detector retinal ganglion cells fire complex spikes and receive only light-evoked inhibition. Proc Natl Acad Sci U S A. 2010; 107:5628–5633. [PubMed: 20212117]

Taghert PH, Bastiani MJ, Ho RK, Goodman CS. Guidance of pioneer growth cones: filopodal contacts and coupling revealed with an antibody to Lucifer yellow. Dev Biol. 1982; 94:391–399. [PubMed: 7152111]

Taylor WR, Vaney DI. Diverse synaptic mechanisms generate direction selectivity in the rabbit retina. J Neurosci. 2002; 22:7712–7720. [PubMed: 12196594]

van Wyk M, Taylor WR, Vaney DI. Local edge detectors: a substrate for fine spatial vision at low temporal frequencies in rabbit retina. J Neurosci. 2006; 26:13250–13263. [PubMed: 17182775]

Vaney DI. Territorial organization of direction-selective ganglion cells in rabbit retina. J Neurosci. 1994; 14:6301–6316. [PubMed: 7965037]

Vaney DI, Levick WR, Thibos LN. Rabbit retinal ganglion cells. Receptive field classification and axonal conduction properties. Exp Brain Res. 1981; 44:27–33. [PubMed: 6168481]

Völgyi B, Chheda S, Bloomfield SA. Tracer coupling patterns of the ganglion cell subtypes in the mouse retina. J Comp Neurol. 2009; 512:664–687. [PubMed: 19051243]

Wässle H, Boycott BB, Illing RB. Morphology and mosaic of on-and off-beta cells in the cat retina and some functional considerations. Proc R Soc Lond B Biol Sci. 1981; 212:177–195. [PubMed: 6166013]

Werblin FS, Dowling JE. Organization of the retina of the mudpuppy, *Necturus maculosus*. II. Intracellular recording. J Neurophysiol. 1969; 32:339–355. [PubMed: 4306897]

Yamada ES, Bordt AS, Marshak DW. Wide-field ganglion cells in macaque retinas. Vis Neurosci. 2005; 22:383–393. [PubMed: 16212697]

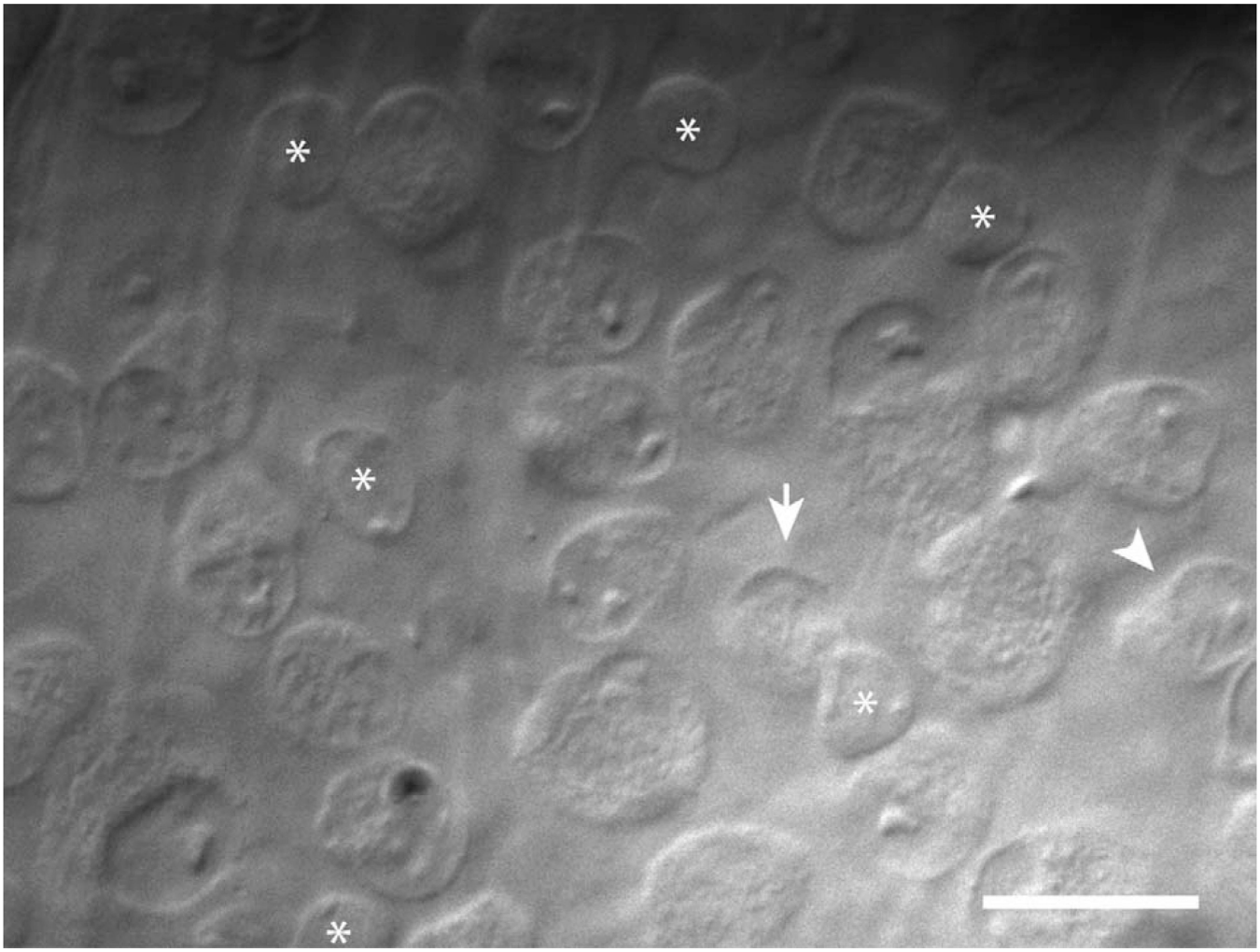

Figure 1.
Microscopic targeting of transient ON-OFF RGCs. Gradient-contrast optics micrograph of the RGC layer in the visual streak of the isolated rabbit retina. The arrow marks a small, round soma that is typical of transient ON-OFF RGCs. Displaced starburst amacrine cells are also numerous in the RGC layer but have slightly smaller somas that are almost filled by the nucleus (asterisks). The arrowhead marks a more elongated soma that is typical of a local edge detector RGC. Scale bar = 20 μm.

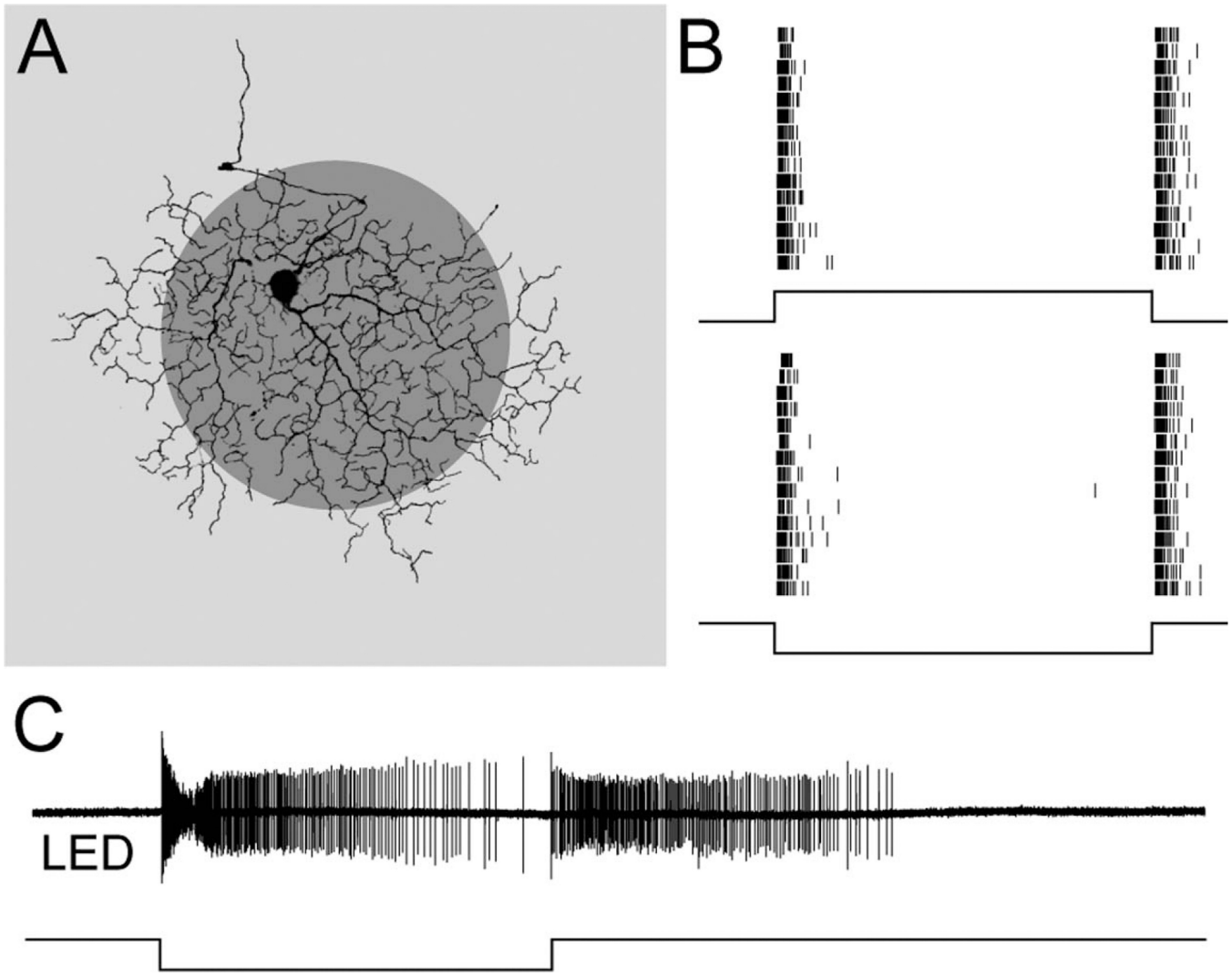

Figure 2.

Extracellular spike responses to flashed stimuli. **A**: The visual stimulus was a 200-μm-diameter dark spot (shown) or light spot (not shown) of 50% contrast, flashed for 2 seconds in the center of the receptive field; the background illumination was in the photopic range. **B**: Spike raster plots from a transient ON-OFF RGC in response to 15 presentations of a bright spot (top) and a dark spot (bottom): the cell fires transiently at both light ON and light OFF. **C**: Spike recording from a local edge detector in response to a dark spot flashed for 6 seconds: the cell gives sustained responses at both light ON and light OFF.

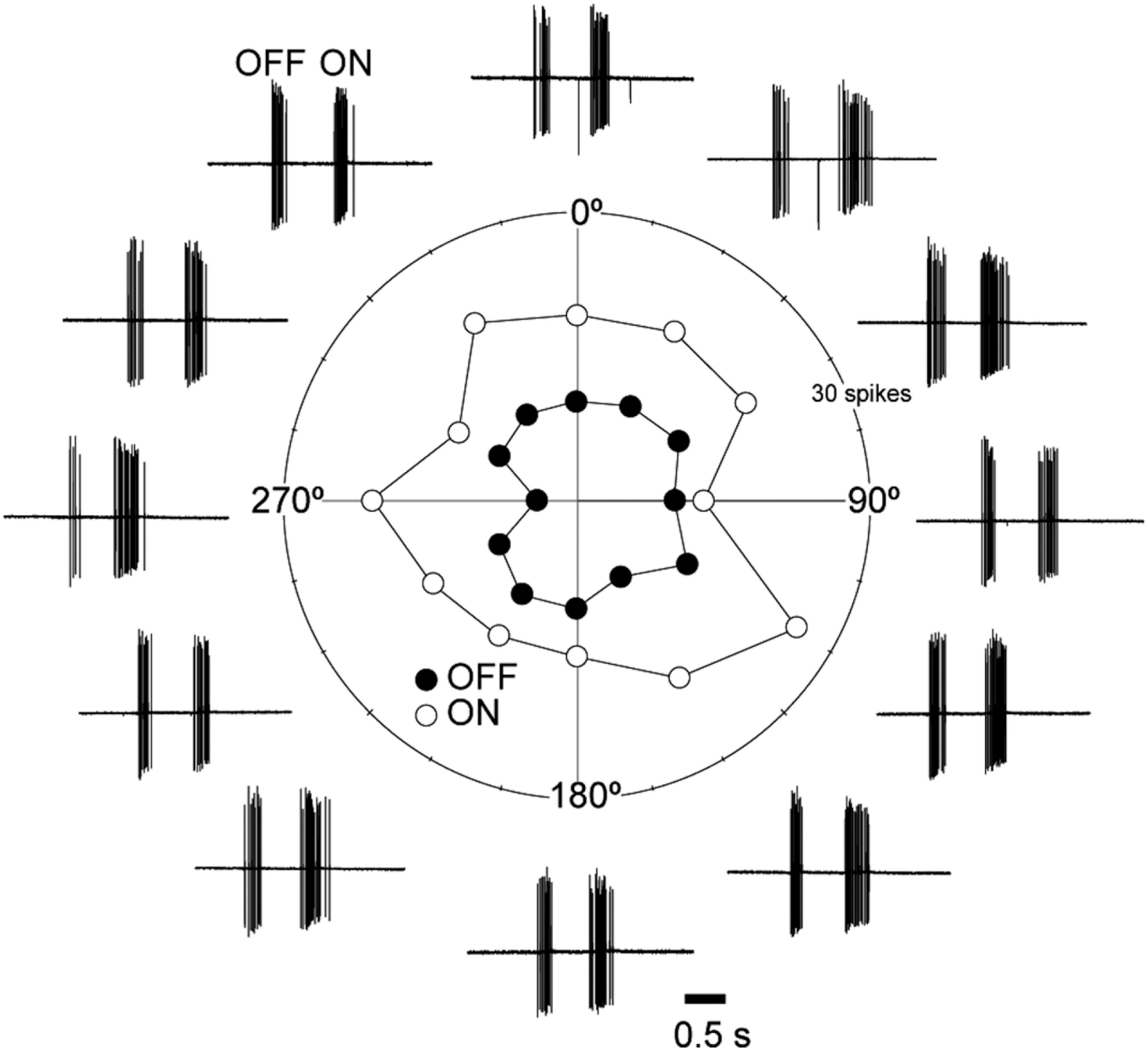

Figure 3.
Transient ON-OFF RGCs are not direction-selective. Polar plot of the spike responses to a dark bar moved through the receptive field in 12 directions spaced at 30° intervals; the first group of spikes to the leading edge is the OFF response (solid circles), and the second group of spikes to the trailing edge is the ON response (open circles).

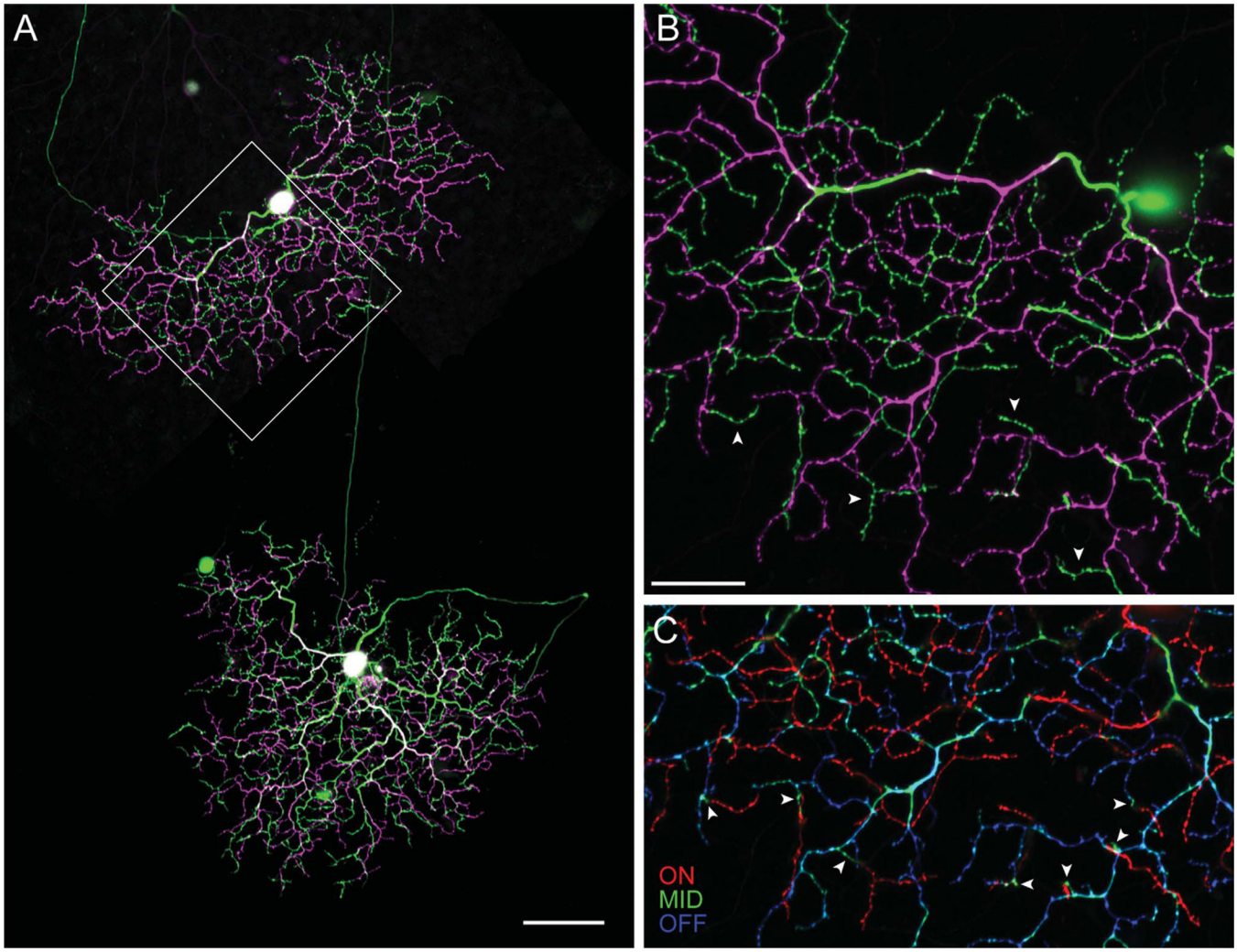

Figure 4.

Dendritic morphology of transient ON-OFF RGCs. **A**: Two adjacent transient ON-OFF RGCs in the visual streak labeled with Neurobiotin following physiological identification. Both cells have densely branched bistratified dendritic trees, with dendrites in the ON sublamina (green) arising from a more dense stratification in the OFF sublamina (magenta). **B**: High-power image of the boxed area in A, illustrating that the ON arbor (green) is formed from short dendrites (arrowheads) arising from the OFF arbor (magenta). **C**: The confocal z-projection shown in B is split into three levels: OFF dendrites in blue, ON dendrites in red, and intermediate dendrites in green. This representation emphasizes the steep vertical branching between the OFF and the ON arbors, as evident in the punctate green profiles (arrowheads), which mark transitions between the two arbors. Scale bar = 100 μm in A; 20 μm in B (applies to B,C).

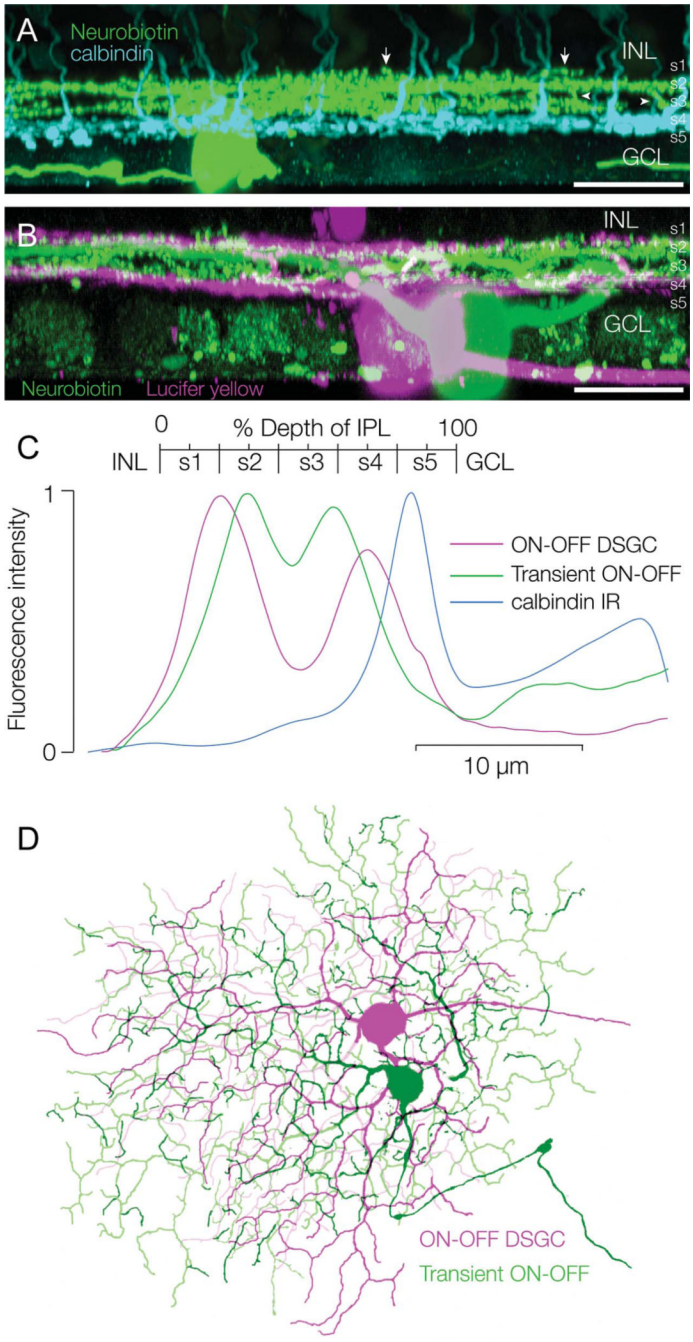

Figure 5.

Stratification of transient ON-OFF RGCs. **A**: Side projection of a transient ON-OFF RGC labeled with Neurobiotin (green) following physiological identification. The retina is double labeled with an antibody against calbindin, which labels a population of bipolar cells (cyan). The RGC dendrites are bistratified and located above the axon terminals of the calbindin bipolar cells, which branch around the S4/S5 border. The ON and OFF arbors in S3 and S2 interconnect through vertical branches (arrowheads) and some OFF dendrites branch in S1, above the main OFF arbor (arrows). **B**: Side projection of a transient ON-OFF RGC labeled with Neurobiotin (green) and an overlapping ON-OFF DSGC labeled with Lucifer yellow

(magenta); the arbors of the transient ON-OFF RGC stratify between the arbors of the ON-OFF DSGC. **C**: Mean fluorescence taken from z-sections through the ON-OFF DSGC (magenta) and transient ON-OFF RGC (green) in B and though the calbindin bipolar cells in A. **D**: Confocal reconstruction of overlapping dye-filled RGCs shows that the dendritic tree of the transient ON-OFF RGC (green) is slightly larger than that of the ON-OFF DSGC (magenta). Scale bars = 50 μm.

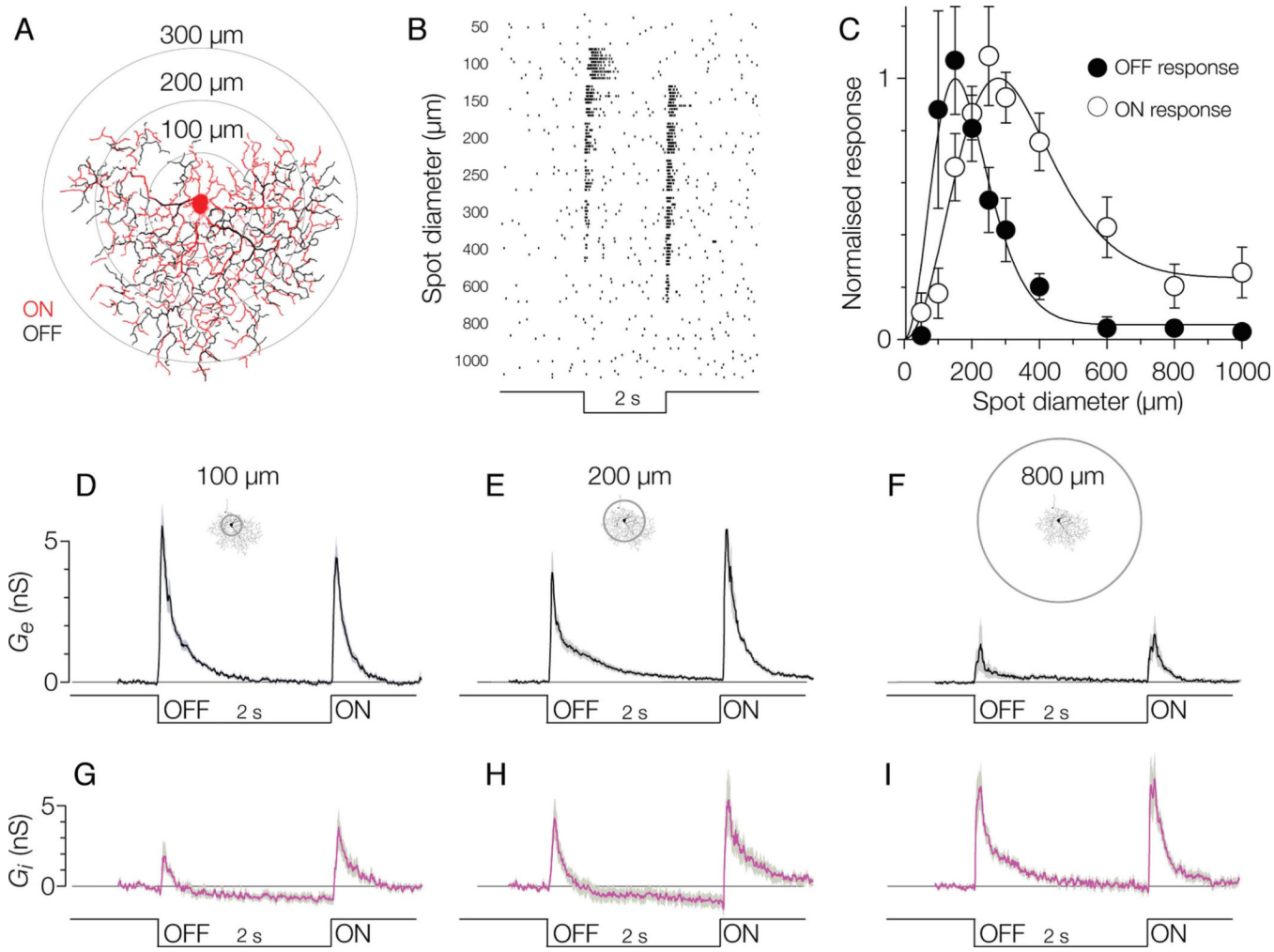

Figure 6.

Physiology of the receptive-field surround. **A**: Flashing-spot stimulation of a transient ON-OFF RGC showing the position of three of the 10 spots relative to the ON (red) and OFF (black) dendritic arbors. **B**: Spike raster plots from the cell shown in A to 10 spots of 50–1,000-µm diameter. **C**: Area-response plots from seven cells to the same stimuli as B, error bars = s.e.m. **D–F**: Excitatory conductance, *Ge* ± s.e.m., averaged from 10 cells in response to a 100-µm spot (D), a 200-µm spot (E), and an 800-µm spot (F). **G–I**: Inhibitory conductance, *Gi* ± s.e.m., averaged from 10 cells in response to a 100-µm spot (G), a 200-µm spot (H), and an 800-µm spot (I).

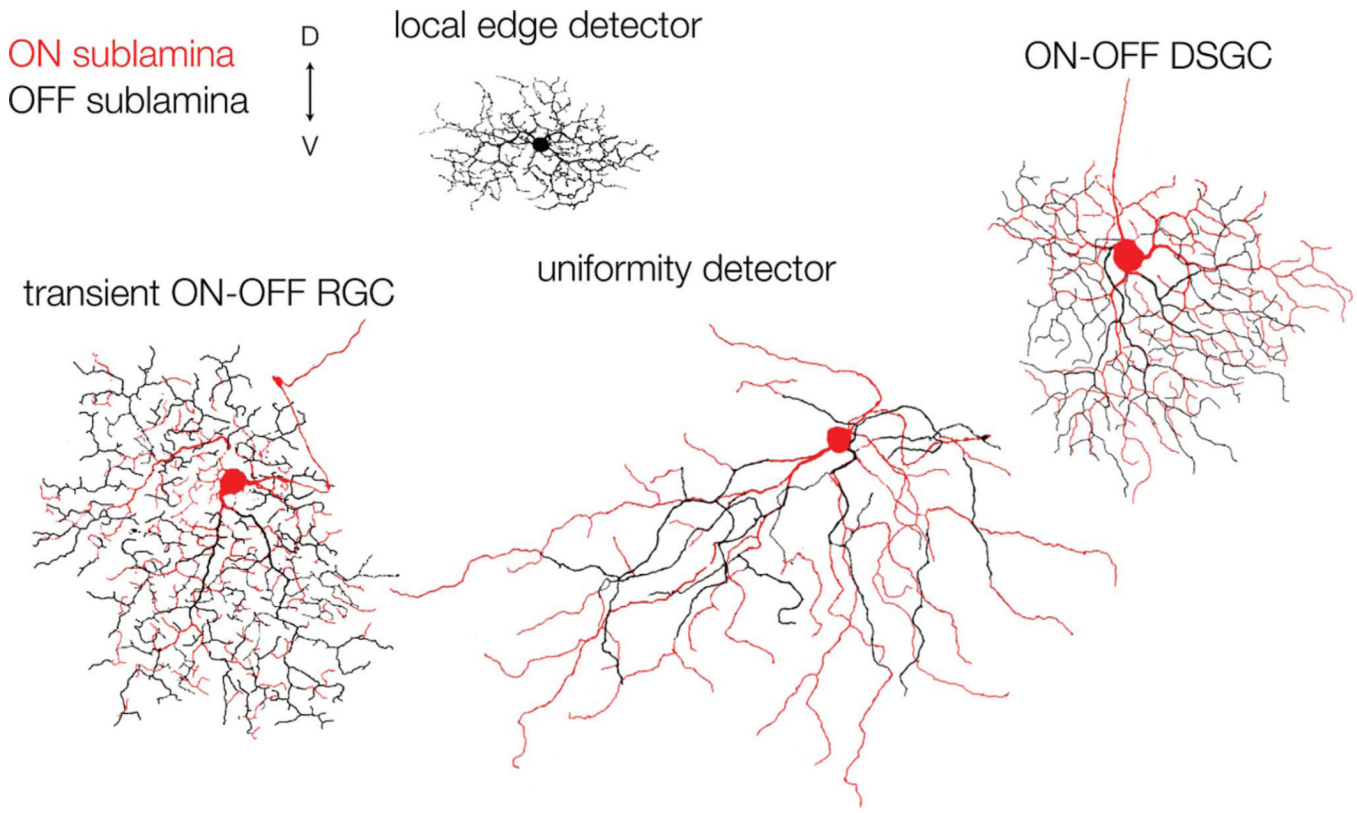

Figure 7.
Dendritic morphology of ON-OFF RGCs in the visual streak of the rabbit retina. The dendritic trees were reconstructed by tracing confocal projections of Neurobiotin-filled RGCs; the ON arbor is shown in red, and the OFF arbor is shown in black. The local edge detector, shown in black, stratifies at the border of the ON and OFF sublaminae. D, dorsal; V, ventral. Scale bar = 100 μm.

TABLE 1

Primary Antisera

Antigen	Dilution	Host species	Supplier	Catalog No.	Immunogen
Calbindin d-28k	1:2,000	Rabbit	Swant	CB 38	Recombinant rat calbindin d-28k
Lucifer yellow	1:10,000	Rabbit	Invitrogen	A5750	Lucifer yellow